Computers and Structures 168 (2016) 30–45

Contents lists available at ScienceDirect

Computers and Structures

journal homepage: www.elsevier.com/locate/compstruc

Sequential surrogate modeling for efficient finite element model updating

Seung-Seop Jin, Hyung-Jo Jung *

Department of Civil and Environmental Engineering, KAIST, Daejeon 305-701, Republic of Korea

ARTICLE INFO

Article history:
Received 7 October 2015
Accepted 10 February 2016
Available online 4 March 2016

Keywords:
Finite element model updating
Surrogate model
Non-stationary response-surface
Kriging model
Sequential modeling

ABSTRACT

Despite the numerous studies concerning finite element model updating (FEMU), a challenging computational cost issue persists. Therefore, surrogate modeling has recently gained considerable attention in FEMU. Conventionally, surrogate models are constructed by identical samples for all outputs. It is very inefficient and subjective, if various response-surfaces exhibit even for identical parameters. Accordingly, we propose a sequential surrogate modeling for FEMU. It uses infill criteria to guide sampling for updating surrogate models automatically. The proposed method is successful to construct the different response-surfaces and apply FEMU. It is promising for constructing surrogate models with minimal user intervention and tremendous computational efficiency.

1. Introduction

Considering that current design and assessment procedures do not have any quantitative linkage to actual existing structures [1], a process to associate physical models with corresponding existing structures is necessary for the condition assessment.

Finite element (FE) model updating is a representative of such a process, and is based on the inverse problem of identifying structural parameters by refining an initial FE model based on experimental data. FE model updating can be categorized into deterministic and non-deterministic approaches. In the deterministic approach [2–5], a residual between measured and computed reference properties is used as an objective function, and an iterative optimization scheme is employed to minimize the objective function by adjusting the model parameters; whereas, the non-deterministic approach takes into account the uncertainties associated with modeling and incomplete measurement data [6–11]. This approach involves finding the most probable models based on the measured data, using a Bayesian statistical framework, and interval and gap analysis.

The most important task in FE model updating is to minimize the systematic error in the FE model. Many engineers prefer using simple approaches owing to their computational efficiency, despite the availability of much more sophisticated modeling approaches [1]. Many researchers have noted that such simple modeling approaches are inadequate, because of their inability to accurately simulate the actual behavior of real structures. Such simple modeling approaches may results in the systematic errors due to modeling simplifications [12], the omission of structural components [13], and FE discretization errors [14]. It is obvious that the presence of systematic errors results in bias in the model prediction, and this leads to incorrect estimations of the updating parameter [15]. Depending on the modeling and our experience, a high-fidelity FE model can increase the required computational time from only seconds to minutes for a simple analysis (e.g., modal analysis). For a single run, this would not be demanding. However, if the FE analysis must be iterated many times, the resulting process would be highly computational-resource intensive.

In this context, surrogate models have recently attracted considerable attention as faster alternatives to the iterative FE analyses. Surrogate modeling is a method of emulating a computer simulation model in the form of a mathematical/statistical approximation, using the input and output of an FE analysis. The fundamental concept of applying surrogating model to reliability analysis is not entirely new. However, the use of surrogate models for FE model updating has been investigated recently, especially in the civil engineering community [16]. Some examples of surrogate models that have so far been investigated are Multilayer perception [17], polynomial model [16,18–20], moving least square method for a polynomial model [21]; radial basis function [22]; Kriging model [23]. Surrogate models are constructed by training samples in the parameter space; therefore, generating the samples for the construction of a surrogate model is a key task. Consequently, conventional surrogate modeling for FE model updating has been investigated from a design of experiments (DOE) in the

* Corresponding author. Tel.: +82 42 350 3626.
E-mail address: hjung@kaist.ac.kr (H.-J. Jung).

http://dx.doi.org/10.1016/j.compstruc.2016.02.005
0045-7949/

previous studies, such as central composite design [16,18,21,22], uniform design [20], D-optimal design [19], and Sobol sequence sampling [23].

The conventional approach generally employs a trial-and-error method based on different designs (i.e., different subsets) of the training samples, because the response-surface is not known beforehand. It is also difficult to represent complicated response-surfaces in the conventional approach under local variations of response behaviors and non-linearity, because the conventional approach generates samples that spread out uniformly across the parameter space. In addition, it is inefficient to apply the identical training samples to all target outputs, if identical updating parameters of the FE model can generate the different response-surfaces of the target outputs due to their relative sensitivity.

To address the abovementioned difficulties, we propose a sequential surrogate (SS) modeling for the efficient FE model updating based on the Kriging model. The proposed method is able to address the abovementioned difficulties of the conventional approach. One crucial advantage of the proposed method is the ability to statistically interpret the uncertainty in the prediction, so that this approach can use the measure of infill criteria and update a surrogate model by adding a new sample.

The rest of this paper is organized as follows. In Section 2, we first describe the mathematical background of the Kriging model, including the statistical interpretation of the Kriging prediction. Next, we present a conventional sequential surrogate modeling originated from the global optimization community [24,25], and a potential problem in FE model updating is discussed. In order to address the potential problem, we propose a sequential surrogate modeling for FE model updating. In Section 3, FE model updating based on the Kriging model with the proposed method is performed numerically and experimentally, using a lab-scaled five-story shear building structure. In addition, the computational efficiency is discussed. In Section 4, we provide concluding remarks on the study.

2. Sequential surrogate modeling based on Kriging model

2.1. Kriging model

The Kriging model is a surrogate model that originated from Geostatistics [26]. The Kriging model is a way of modeling a function as a realization of Gaussian process. Assuming that the function being modeled is continuous, two samples of the true function will tend to have similar values if the distance between the two samples decreases. This spatial correlation can be used to estimate an unknown function value from the known function values. This property can be given the statistical interpretation that the values of the function are correlated with a spatial distance. Therefore, this spatial correlation can be modeled statistically, using the relative distances between the samples. The k-dimensional Kriging basis can be expressed as

$$\psi^{ij} = \exp\left(-\sum_{p=1}^{k}\theta_p\left\|x_p^i - x_p^j\right\|^{m_p}\right) = corr\left[y(\boldsymbol{x}^i), y(\boldsymbol{x}^j)\right] \tag{1}$$

where subscript "p" denotes the dimension of sample x, the superscripts "i" and "j" indicate the ith and jth sample, respectively, and $\left\|x^i - x^j\right\|^{m_p}$ is the relative distance measure between two samples in a parameter space with m-norm. The Kriging basis contains parameters corresponding to each dimension (θ_p and m_p) that determine how fast the correlation decays in each dimension. Therefore, these parameters serve to reflect the significant importance of each dimension [25]. The main purpose of using this flexible basis is to express the various shapes of the spatial correlation. To reduce the computational complexity, Eq. (1) can be expressed as a Euclidean distance ($m_p = 2$). In the remainder of this paper, boldface indicates a matrix or vector.

2.1.1. Modeling of Kriging model

Using a random vector ($\boldsymbol{Y}$), the values of a function of n samples can be represented as

$$\boldsymbol{Y} = \left[y(\boldsymbol{x}^1)y(\boldsymbol{x}^2)\cdots y(\boldsymbol{x}^n)\right]^T \tag{2}$$

This random vector ($\boldsymbol{Y}$) has a mean of $\boldsymbol{1}\mu$, where $\boldsymbol{1}$ is an n-by-1 unit vector, and a variance of σ^2. Assuming that the realizations ($y(\boldsymbol{x})$) of this random vector are correlated, the correlation function can be defined as in Eq. (1), using a 2-norm ($m_p = 2$). Therefore, the correlation matrix of all samples can be constructed as

$$\boldsymbol{\Psi} = corr[\boldsymbol{Y},\boldsymbol{Y}] = \begin{bmatrix} corr\left[y(\boldsymbol{x}^1), y(\boldsymbol{x}^1)\right] & \cdots & corr\left[y(\boldsymbol{x}^1), y(\boldsymbol{x}^n)\right] \\ \vdots & \ddots & \vdots \\ corr\left[y(\boldsymbol{x}^n), y(\boldsymbol{x}^1)\right] & \cdots & corr\left[y(\boldsymbol{x}^n), y(\boldsymbol{x}^n)\right] \end{bmatrix} \tag{3}$$

The covariance matrix can be derived from the correlation matrix ($\boldsymbol{\Psi}$), as

$$COV(\boldsymbol{Y},\boldsymbol{Y}) = \sigma^2\boldsymbol{\Psi} \tag{4}$$

The variance σ^2 determines the overall dispersion relative to the mean of the Kriging model.

The value of the function represents the realization of the Gaussian process, so that μ and σ^2 are estimated using the observed pattern of the training samples.

In a similar manner to statistical estimation theory, the parameters are estimated using maximum likelihood estimation. The likelihood function is given by

$$L = \frac{1}{(2\pi\sigma^2)^{n/2}|\boldsymbol{\Psi}|^{1/2}}\exp\left[-\frac{(\boldsymbol{Y}-\boldsymbol{1}\mu)^T\boldsymbol{\Psi}^{-1}(\boldsymbol{Y}-\boldsymbol{1}\mu)}{2\sigma^2}\right] \tag{5}$$

To simplify the likelihood function with numerical stability, the natural logarithm of Eq. (5) is taken, and the constant term is then ignored. Therefore, we obtain

$$\ln(L) \approx -\frac{n}{2}\ln\left(\sigma^2\right) - \frac{1}{2}\ln|\boldsymbol{\Psi}| - \frac{(\boldsymbol{Y}-\boldsymbol{1}\mu)^T\boldsymbol{\Psi}^{-1}(\boldsymbol{Y}-\boldsymbol{1}\mu)}{2\sigma^2} \tag{6}$$

By taking the derivatives of Eq. (6) with respect to μ and σ^2 and setting these to zero, the maximum likelihood estimators for μ and σ^2 are derived as follows:

$$\hat{\mu} = \frac{\boldsymbol{1}^T\boldsymbol{\Psi}^{-1}\boldsymbol{Y}}{\boldsymbol{1}^T\boldsymbol{\Psi}^{-1}\boldsymbol{1}} \tag{7}$$

$$\hat{\sigma}^2 = \frac{(\boldsymbol{Y}-\boldsymbol{1}\mu)^T\boldsymbol{\Psi}^{-1}(\boldsymbol{Y}-\boldsymbol{1}\mu)}{n} \tag{8}$$

By substituting Eqs. (7) and (8) into Eq. (6) and ignoring the constant terms, we obtain the so-called concentrated log-likelihood function, as

$$\ln(L) \approx -\frac{n}{2}\ln\left(\hat{\sigma}^2\right) - \frac{1}{2}\ln|\boldsymbol{\Psi}| \tag{9}$$

It is not possible to differentiate Eq. (9). However, it is obvious that maximum likelihood estimates ($\hat{\mu}$ and $\hat{\sigma}^2$) can be sequentially computed from the correlation matrix ($\boldsymbol{\Psi}$) and the training samples, so that the only remaining parameter to be determined in Eq. (1) is θ_p. Therefore, an optimization method is applied to find the optimal θ_p by maximizing Eq. (9).

2.1.2. Prediction of Kriging model

Let $(\boldsymbol{x}^*, \hat{y})$ denote the new sample and its prediction, and let the new augmented values of the function $(\widetilde{\boldsymbol{Y}})$ with the new prediction $(\hat{y})$ be defined by

$$\widetilde{\boldsymbol{Y}} = \begin{bmatrix} \boldsymbol{Y}^T & \hat{y} \end{bmatrix}^T \tag{10}$$

Furthermore, the vector of correlation between the new sample $(\boldsymbol{x}^*)$ and the training samples $(\boldsymbol{x}^i)$ is defined by

$$\hat{\boldsymbol{\psi}} = \begin{pmatrix} corr\left[y(\boldsymbol{x}^*), y(\boldsymbol{x}^1)\right] & \cdots & corr\left[y(\boldsymbol{x}^*), y(\boldsymbol{x}^n)\right] \end{pmatrix}^T \tag{11}$$

From the definition of the correlation matrix $(\boldsymbol{\Psi})$ in Eq. (3), the augmented correlation matrix $(\widetilde{\boldsymbol{\Psi}})$ can be constructed as

$$\widetilde{\boldsymbol{\Psi}} = \begin{pmatrix} \boldsymbol{\Psi} & \hat{\boldsymbol{\psi}} \\ \hat{\boldsymbol{\psi}} & \mathbf{1} \end{pmatrix} \tag{12}$$

where $\mathbf{1}$ is the unit vector. Except for the last term in Eq. (6), all other terms are constant, because they are already determined in the maximum likelihood estimation under the training samples. In other words, the last term in Eq. (6) is the only variable in maximizing the likelihood. Therefore, the augmented log-likelihood function in the Kriging prediction becomes

$$\ln\left(L(\hat{\mu}, \hat{\sigma})\right) \approx -\frac{\left(\widetilde{\boldsymbol{Y}} - \mathbf{1}\hat{\mu}\right)^T \widetilde{\boldsymbol{\Psi}}^{-1}\left(\widetilde{\boldsymbol{Y}} - \mathbf{1}\hat{\mu}\right)}{2\hat{\sigma}^2} \tag{13}$$

By substituting Eqs. (10) and (12) into Eq. (13) and using the partitioned inverse formula [27], only the terms relating to $\hat{y}$ remain, and the augmented log-likelihood becomes

$$\ln\left(L(\hat{\mu}, \hat{\sigma})\right) \approx \left(\frac{-1}{2\hat{\sigma}^2\left(1 - \hat{\boldsymbol{\psi}}^T\boldsymbol{\Psi}^{-1}\hat{\boldsymbol{\psi}}\right)}\right)(\hat{y} - \hat{\mu})^2 + \left(\frac{\hat{\boldsymbol{\psi}}^T\boldsymbol{\Psi}^{-1}(Y - 1\hat{\mu})}{\hat{\sigma}^2\left(1 - \hat{\boldsymbol{\psi}}^T\boldsymbol{\Psi}^{-1}\hat{\boldsymbol{\psi}}\right)}\right) \times (\hat{y} - \hat{\mu}) \tag{14}$$

The prediction $(\hat{y})$ should maximize the augmented log-likelihood. By differentiating with respect to $\hat{y}$, the prediction of the Kriging model (i.e., the Kriging predictor) is

$$\hat{y}(\boldsymbol{x}^*) = \hat{\mu} + \boldsymbol{\psi}^T\boldsymbol{\Psi}^{-1}(\boldsymbol{Y} - \mathbf{1}\hat{\mu}) \tag{15}$$

2.2. Sequential surrogate modeling based on statistical interpretation

The basic concept of the sequential surrogate modeling is presented in Fig. 1. The sequential surrogate modeling adds a new sample, which has high likelihood of improvement based on the statistical interpretation of the prediction, to improve the accuracy of the surrogate model and reduce the variance. In this subsection, the statistical interpretation of prediction is first described, and then a conventional sequential surrogate modeling originated from the global optimization community [24,25] is discussed with a potential problem in FE model updating. Lastly, the proposed method is presented for FE model updating.

2.2.1. Statistical interpretation of Kriging prediction

After estimating the mean $(\hat{\mu})$ and variance $(\hat{\sigma}^2)$ of the Kriging model from the training samples, the augmented log-likelihood function (Eq. (14)) is the function of the prediction $(\hat{y})$. The uncertainty of the prediction is interpreted by Eq. (14). Because this is a second-order polynomial function of the prediction $(\hat{y})$, the shape of the augmented log-likelihood function is parabolic, with two possible types of curvature. A higher curvature results in a sharper shape around the maximum value, while a lower curvature results in a smoother and flatter shape around the maximum value.

In this regard, the statistical interpretation of the prediction can evaluate the potential uncertainty of the Kriging prediction based on the curvature of the augmented log-likelihood function. Therefore, the uncertainty of the Kriging prediction is estimated by taking the second derivative of the augmented log-likelihood function, as follows:

$$\frac{\partial^2\left(ln(L(\hat{\mu}, \hat{\sigma}))\right)}{\partial^2\hat{y}} \approx \frac{-1}{\hat{\sigma}^2\left(1 - \hat{\boldsymbol{\psi}}^T\boldsymbol{\Psi}^{-1}\hat{\boldsymbol{\psi}}\right)} \tag{16}$$

The denominator in Eq. (16) is used as the measure of uncertainty in the prediction. This is very similar to the mean squared error (MSE) of the predictor in the Gaussian process [28].

$$\hat{s}^2(y(\boldsymbol{x}^*)) = \hat{\sigma}^2\left(1 - \hat{\boldsymbol{\psi}}^T\boldsymbol{\Psi}^{-1}\hat{\boldsymbol{\psi}}\right) \tag{17}$$

As shown in Fig. 2a, the prediction at any point is modeled as the stochastic realization with a mean of $(\hat{y}(\boldsymbol{x}^*))$ and MSE of $(\hat{s}^2(y(\boldsymbol{x}^*)))$, from Eqs. (15) and (17) respectively, so that the Kriging model can statistically interpret the measure of uncertainty in each prediction.

2.2.2. Expected improvement and typical sequential modeling for global optimization

The expected improvement (EI) approach gives criteria for evaluating how much improvement in current best value $I(\boldsymbol{x}^*)$ is expected if a new sample is obtained [24,25]. In this approach, $y(\boldsymbol{x}^*)$ is treated as a Gaussian random variable with mean $(\hat{y}(\boldsymbol{x}^*))$ and variance $(\hat{s}^2(y(\boldsymbol{x}^*)))$, as shown in Fig. 2a. If the current best value is $y_{\min}$, then $I(\boldsymbol{x})$ is defined as

$$I(\boldsymbol{x}) = y_{min} - Y(\boldsymbol{x}^*) \tag{18}$$

This is estimated by a Gaussian density function with mean $(\hat{y}(\boldsymbol{x}^*))$ and variance $(\hat{s}^2(y(\boldsymbol{x}^*)))$:

$$\phi(\boldsymbol{x}^*) = \frac{1}{\sqrt{2\pi\hat{s}^2(y(\boldsymbol{x}^*))}} \exp\left[-\frac{\left(Y(\boldsymbol{x}^*) - \hat{y}(\boldsymbol{x}^*)\right)^2}{2\hat{s}^2(y(\boldsymbol{x}^*))}\right] \tag{19}$$

Substituting Eq. (18) into Eq. (19) gives

$$\phi(\boldsymbol{x}^*) = \frac{1}{\sqrt{2\pi\hat{s}^2(y(\boldsymbol{x}^*))}} \exp\left[-\frac{\left(y_{min} - I(\boldsymbol{x}^*) - \hat{y}(\boldsymbol{x}^*)\right)^2}{2\hat{s}^2(y(\boldsymbol{x}^*))}\right] \tag{20}$$

By integrating Eq. (20) with respect to $I(\boldsymbol{x}^*)$, we obtain the EI as

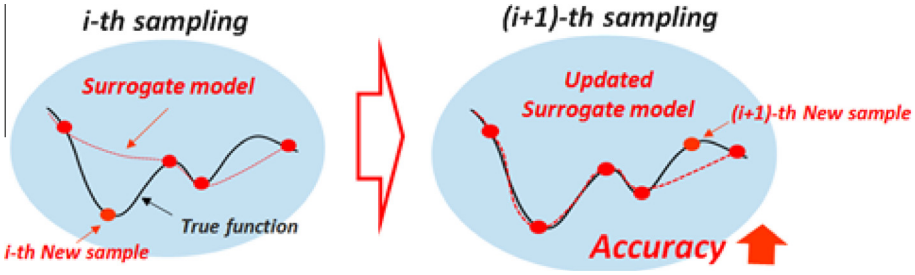

Fig. 1. Concept of sequential surrogate modeling.

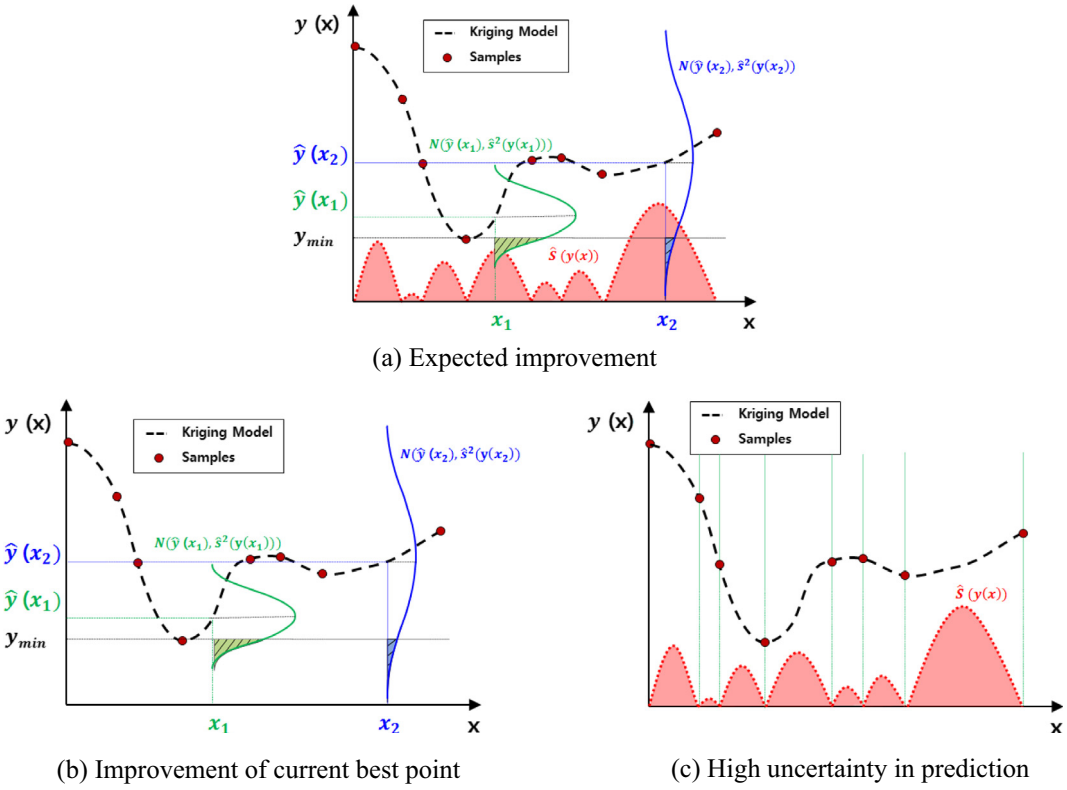

(a) Expected improvement

(b) Improvement of current best point

(c) High uncertainty in prediction

Fig. 2. Expected improvement in Kriging model.

$$E[I(\boldsymbol{x}^*)] = \int_0^\infty I(\boldsymbol{x}^*) \cdot \left\{ \frac{1}{\sqrt{2\pi\hat{s}^2(y(\boldsymbol{x}^*))}} \exp\left[-\frac{(y_{min} - I(\boldsymbol{x}^*) - \hat{y}(\boldsymbol{x}^*))^2}{2\hat{s}^2(y(\boldsymbol{x}^*))} \right] \right\} dI \tag{21}$$

By using integration by parts, we evaluate

$$E[I(\boldsymbol{x})] = (y_{min} - \hat{y}(\boldsymbol{x}^*)) \left[\frac{1}{2} + \frac{1}{2} \mathrm{erf}\left(\frac{y_{min} - \hat{y}(\boldsymbol{x}^*)}{\hat{s}(y(\boldsymbol{x}^*))\sqrt{2}} \right) \right] + \hat{s}(y(\boldsymbol{x}^*)) \frac{1}{\sqrt{2\pi}} \exp\left[-\frac{y_{min} - \hat{y}(\boldsymbol{x}^*)^2}{2\hat{s}^2(y(\boldsymbol{x}^*))} \right] \tag{22}$$

where $\mathrm{erf}(\cdot)$ denotes the error function that is generally used for the cumulative Gaussian distribution. As shown in Fig. 2b, the first term in Eq. (22) tends to be larger when the prediction is likely to be better than the current best value (i.e., exploitation), while the second term tends to be larger when there is a higher uncertainty in the prediction ($\hat{s}(y(\boldsymbol{x}^*))$), as shown in Fig. 2c (i.e., exploration).

The flowchart of the typical sequential surrogate (SS) modeling for the global optimization is presented in Fig. 3a, and can be described as follows:

1. Generate initial samples by DOE with upper and lower bounds of parameters.
2. Run FE analysis based on initial samples.
3. Construct the Kriging model from the current training samples and evaluate the stopping criteria (Eq. (23)).
4. If the stopping criteria are not met, find an additional sample numerically, based on EI. After obtaining a sample for infill, FE analysis of this sample is performed and added to the current training samples. Finally, go to Step 3 and repeat the loop, until the stopping criteria is met. Otherwise, stop the sequential modeling.

The following general stopping strategy is used to stop the sequential surrogate modeling when the relative change of the Euclidean distance between the number of successive and additional samples is small [24,25,29].

$$\|x_i - x_{i-1}\| \leqslant \Delta X_{TOL} \tag{23}$$

where $\|\cdot\|$ is the Euclidean distance between consecutive samples (x_{i-1} and x_i), and ΔX_{TOL} denotes the tolerance for termination. This was originally developed in order to find the optimum within a minimal number steps in a computationally expensive simulation.

It is very important to assess the adequacy of the Kriging model before using it as a fast surrogate. Owing to an undesirable stop, the typical SS modeling may provide Kriging models with significant errors in the prediction. This problem will be illustrated in Section 2.2.4. Due to the nature of the Kriging model (i.e., interpolation), the outputs on the training samples are exactly the same as the corresponding predictions of the Kriging model. For this reason, additional samples (i.e., validation samples) are typically required to evaluate the adequacy after constructing the Kriging model [30].

2.2.3. Proposed sequential surrogate modeling based on validation samples

Unlike the conventional surrogate modeling and typical SS modeling, the proposed method utilizes the validation samples in the modeling phase. This is originated from a traditional validation test, using independent samples that are not used in constructing the surrogate model. By virtue of using validation samples, the proposed method can omit the phase of model diagnostic and address an undesirable stop due to the deceptive training samples. This section presents the proposed method with the guideline for the validation samples. The guideline is presented firstly, and then the proposed method is introduced.

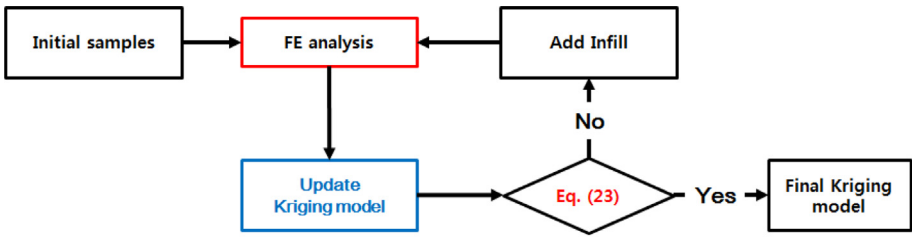

(a) Typical sequential surrogate modeling for global optimization

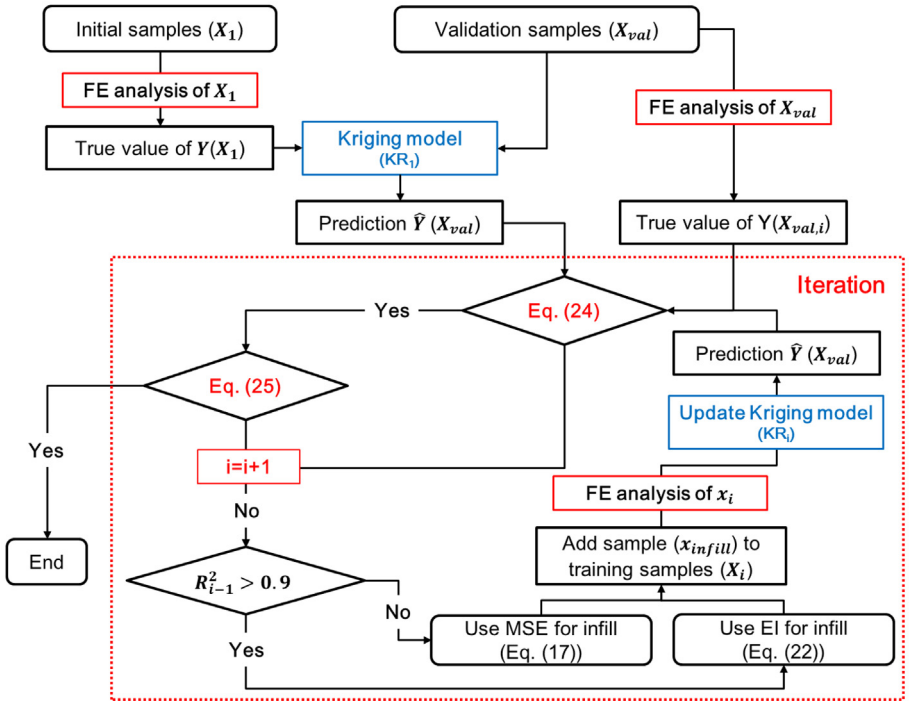

(b) Proposed sequential surrogate modeling for FE model updating

Fig. 3. Sequential surrogate modeling approaches with Kriging model.

Because the response-surfaces of the target outputs are not known in advance, the validation sample design in the proposed method is to obtain the best possible coverage of the parameter space. Therefore, we use an optimized Latin hypercube sampling (LHS) method with an optimality criterion (i.e., Morris–Mitchell criterion [31]) to prevent a potential lack of uniformity [32,33]. An alternative method would be Quasi random sequences techniques [34–37]. No formal guidelines exist for choosing the sample size, so the empirical relation "$N \sim 10d$" is widely employed for space-filling designs [33,38,39]. In Loeppky, Sacks [39], simulation studies are performed in order to demonstrate that this empirical relation gives the approximate minimum sample size for exploring the whole parameter space. Accordingly, we employ this empirical relation for validation samples.

Based on the validation samples, the two common validation measures of R-squared value (R^2) and root mean square error (RMSE) are calculated [40]. R^2 represents a measure of how well the observed outputs are reproduced by the prediction model. A larger value that is close to one is preferred. The RMSE provides an additional measure, as a measure of the squared difference between the observed and predicted outputs in the validation sample. A smaller value that is close to zero indicates a higher accuracy for the prediction.

Based on these validation measures, the two stopping criteria (Eqs. (24) and (25)) are used to determine whether the sequential surrogate modeling stops or not:

$$R_i^2 \geqslant R_{Thresh}^2 \tag{24}$$

$$|RMSE_i - RMSE_{i+1}| \leqslant \Delta RMSE_{Thresh}(1 + |RMSE_i|) \tag{25}$$

where the subscript "i" indicates the ith state of an infill sample, and "*Thresh*" indicates the threshold value. Especially, RMSE may fluctuate greatly at the early stage; therefore there is a risk that the proposed method stops prematurely. To prevent this undesired stop, we introduce a lower bound on the change in the RMSE value (Eq. (25)) as a measure of the convergence. As the approximation becomes closer to the true function, R^2 approaches unity, and the relative change in the RMSE becomes small.

The proposed method uses two infill criteria in an adaptive manner. If R^2 is less than 0.9, MSE is used to find a new sample in a higher uncertain region and add it to training samples for update of the Kriging model. Once reasonable approximation is achieved (i.e., above 0.9 of R^2), EI is used to find a new sample which is highly likely improvement of the Kriging model. The framework of the proposed method is presented in Fig. 3b, and can be described as follows:

1. Generate an initial sample ($\mathbf{X_1}$) and validation samples ($\mathbf{X_{val}}$) using DOE with upper and lower bounds on parameters.
2. Initial sample ($\mathbf{X_1}$) and validation sample ($\mathbf{X_{val}}$) are used as inputs to run the FE analysis to obtain the outputs ($\mathbf{Y}(\mathbf{X_1}), \mathbf{Y}(\mathbf{X_{val}})$).
3. Construct an initial Kriging model ($\mathbf{KR_1}$) based on the training samples ($\mathbf{X_1}$, $\mathbf{Y}(\mathbf{X_1})$).
4. Predict the validation sample outputs ($\widehat{\boldsymbol{Y}}(\mathbf{X_{val}})$) using the initial Kriging model ($\mathbf{KR_1}$).
5. Evaluate the validation measures ($\boldsymbol{R_1^2}$, $\boldsymbol{RMSE_1}$) by Eqs. (24) and (25). Stop if the stopping criteria are met; otherwise, go to Step 6.
6. Determine the infill sample ($\boldsymbol{x_{Infill}}$): If R^2 is less than 0.9, MSE (Eq. (17)) is used for infill. Otherwise, EI (Eq. (22)) is used.
7. Evaluate the true output of the infill ($\mathbf{Y}(\boldsymbol{x_{infill}})$), and update the Kriging model ($\mathbf{KR_i}$).
8. Predict the validation sample outputs ($\widehat{\boldsymbol{Y}}(\mathbf{X_{val,i}})$) using the updated Kriging model ($\mathbf{KR_i}$).
9. Evaluate the validation measures ($\boldsymbol{R_i^2}$, $\boldsymbol{RMSE_i}$) and Eqs. (24) and (25).
10. Stop if the stopping criteria are met; otherwise, return to Step 6.

2.2.4. Motivated example

This subsection presents the comparative study between the typical SS modeling and the proposed method. Through the comparative study, we show the problem of the typical SS modeling and how the validation samples play a role in addressing this problem.

The comparative study is performed with the test function of Eq. (26) with five initial samples. The typical SS modeling was implemented with 0.01 of ΔX_{TOL}, while the proposed method was implemented with 0.95 of R^2_{Th} and 0.01 of $\Delta RMSE_{Th}$. Five samples are used as validation samples for the proposed method.

$$f(x) = x\,\sin(10x+1) + 0.1\sin(15x), \quad x \in [-0.6, 1] \tag{26}$$

Fig. 4 shows the sample paths from the typical and proposed method. Both SS modeling inferred the identical infill samples until 4 infill stages, since they used the same infill criteria to infer the sample. Both SS modeling stay in the neighborhood of the minima at two sequential infill stages (i.e., 1–2 and 3–4 infill stages).

After 4 infill stages, the typical SS modeling judged its convergence impetuously and stops the infill process. As shown in Fig. 5a, typical SS modeling stops with significant error in the prediction. From the viewpoint of global optimization, this is preferable with the minimal function evaluation to find the minimum. Considering that the updated Kriging model replaces an iterative FE analysis in FE model updating, the additional samples are required to evaluate the adequacy of the updated Kriging model in typical SS modeling. On the other hand, the proposed method did not stop the SS modeling by virtue of using validation samples. Until 4 infill stages, four of five validation samples are not matched to those of the prediction. After 8 infill stages, the proposed method stops with 18 total evaluations of the true function (i.e., 5 initial samples, 8 infill samples, and 5 validation samples). Finally, it can construct and update Kriging model as close as true function as shown in Fig. 5b. By using validation samples in the proposed method, the proposed method can remove the phase of model diagnostic and address a problem due to the deceptive training samples.

3. Kriging model-based FE model updating with sequential surrogate modeling

In this section, we evaluate the performance of the method proposed in Section 2 by using a five-story shear building. There are two reasons to use this shear building: Firstly, this shear building is simple and easy to understand; Secondly, it has a variety of the response-surfaces from simple and smooth to complex (i.e., non-stationary) one, even for identical input parameters. Therefore, it is appropriate to describe our motivation and evaluate the performance of the proposed method.

This section is divided into two parts. In the first part, we explain the preliminary preparation of the FE model updating process, such as a description of the target structure and its FE model. In the second part, the proposed method is evaluated by conducting a numerical study and a lab-scaled experiment. Considering that the primary intention of this study is to evaluate the proposed method with surrogate-based FE model updating, concerning potential computational issues with the high-fidelity model, we adopt a deterministic FE model updating approach based on residual minimization, for simplicity.

3.1. Preliminary works for FE model updating

A five-story shear building is used to evaluate the proposed method, as shown in Fig. 6a. The boundary condition for the target structure is clamped, to fix all degrees of freedom. The connections between floors and columns are bolted to each other. The details of the geometric information are presented in Fig. 6b, with an FE model developed using SAP2000. The FE model is constructed from 1273 shell elements with 1384 nodes, to fully represent the geometry of the structure. The ideal fixed condition does not exist in reality. Therefore, the support condition is modeled by a hinge support with a rotational spring in the FE model. By applying a rotational spring, as shown in Fig. 6c, the support condition from the hinge to the fixed support can be represented by the variation of the rotational spring constant, as shown in Fig. 6d. The properties of the structural parameters are listed in Table 1.

3.2. Numerical study

The main objective of this subsection is to accurately evaluate the proposed method. If one of the surrogate models does not accurately approximate the FE model, then FE model updating cannot provide the exact target value under ideal conditions (i.e., no error and uncertainty). For this purpose, we performed the following numerical study.

In order to determine the model properties of the target structure, the initial values of the updating parameters are perturbed. The corresponding modal properties are then obtained from the FE analysis as measured quantities for the numerical study. As shown in Table 2, two updating parameters are perturbed: First, the group of Young's moduli (E^1–E_5), E; Second, the rotational spring at the support condition, K_R. The ranges of the updating parameters are $0.8 \leqslant \Delta E \leqslant 1.2$ and $0.001 \leqslant \Delta K_R \leqslant 2$. There are two reasons for the selection of these two updating parameters. First, it is easy to visualize the response-surfaces. Second, they exhibit more complex response-surfaces relationships under local variations in the response behavior and non-linearity in the lower modal properties. In order to visualize the response-surfaces, a total of 1681 FE analyses were performed, using uniform grid sampling with 41 levels (i.e., 41×41 grid sampling). For the computation of the MAC (modal assurance criterion) values, mode shapes of the target FE model were used as the reference quantity for computing the MAC values with those from the perturbed FE model. Fig. 7 illustrates the response-surfaces of the first three modal properties. The reason why the response-surfaces of the lower modal properties are more complicated is that the sensitivity of K_R is significantly larger for the lower modal properties (see Fig. 13). We also note that the response-surfaces are different for each target modal property even under identical updating

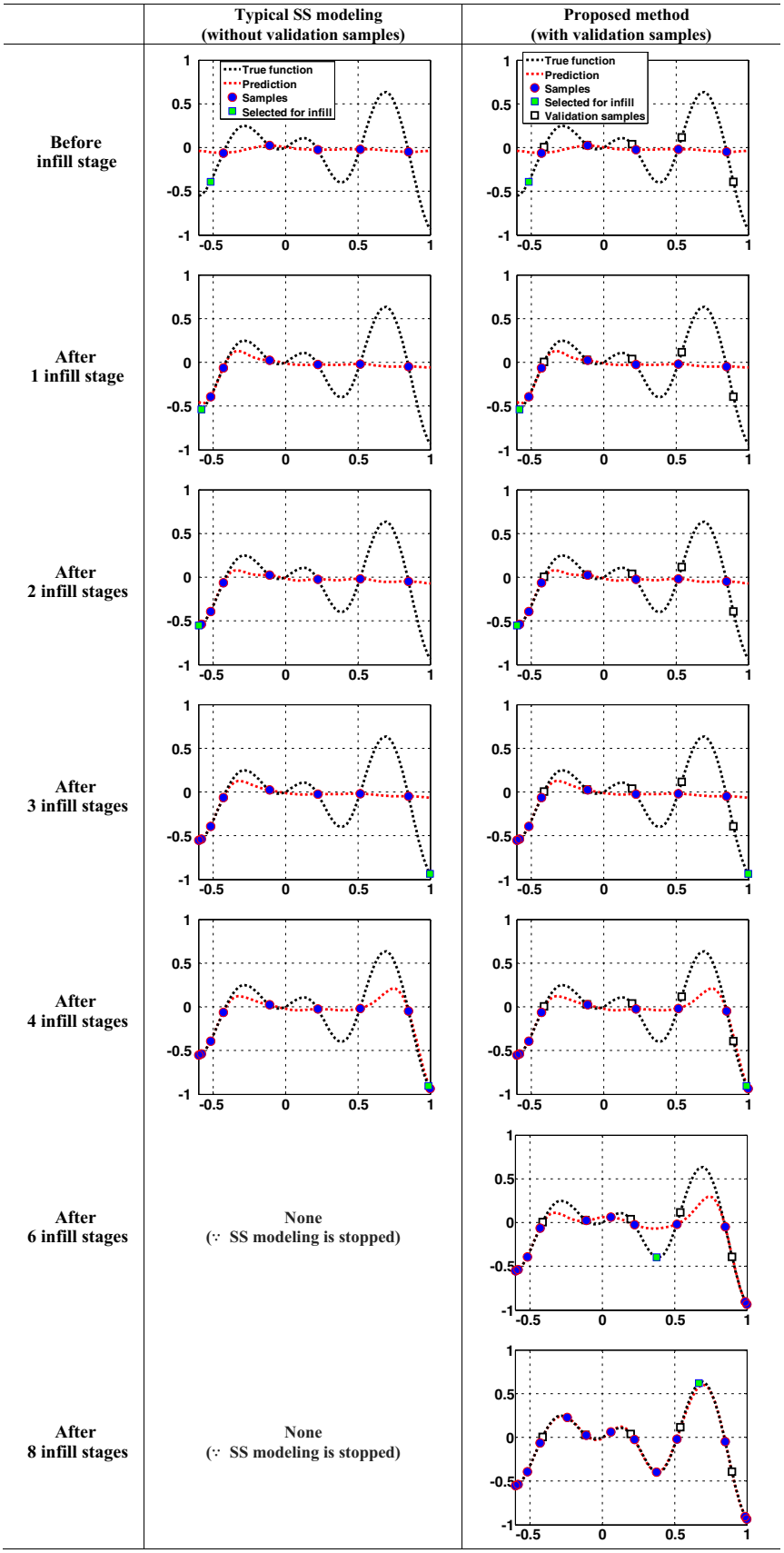

Fig. 4. Comparison between sample paths of typical and proposed sequential surrogate modeling.

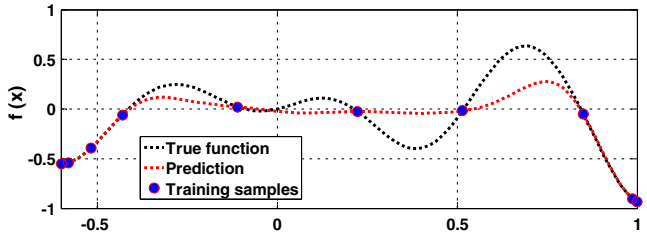

(a) Typical sequential surrogate modeling for global optimization (after 5 infill stages)

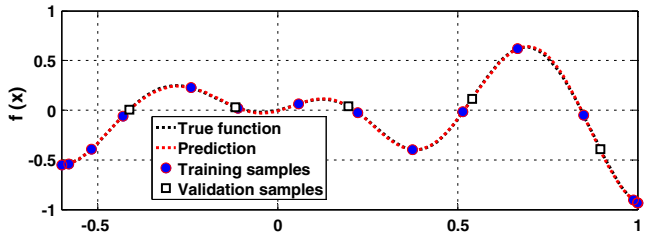

(b) Proposed sequential surrogate modeling for FE model updating (after 9 infill stages)

Fig. 5. Final approximations of the typical and proposed sequential surrogate modeling.

parameters, as shown in Fig. 7, so that the number of samples and their locations should be different to capture this effect accurately. Therefore, the conventional approach using identical training samples for all target outputs is not efficient.

In order to build the initial Kriging model, 10 samples were generated using optimized LHS. As the validation samples, a total of 40 samples were generated by optimized LHS. Because the symptom of non-stationary response-surfaces occurs in the sensitivity analysis (Fig. 13), the validation sample size was increased to 40, based on a minimum sample size of 20 (i.e., $N \sim 10d$).

Subsequently, six Kriging models (i.e., lowest three natural frequencies and MAC values) were constructed using the proposed method. For the stopping criteria, the thresholds of R^2_{Th} and $\Delta RMSE_{Th}$ were set to 0.98 and 0.01, respectively. We note that the proposed method for the target modal properties was initiated independently with 10 initial samples, to show that different training samples are required. The practical implementation of the proposed method is detailed in Section 3.4.

The progress of the proposed method is presented in Fig. 8. As additional samples are incorporated into the training samples, the accuracy of the Kriging model is improved. We observe that the required number of training samples is different for each target modal property. In particular, in the Kriging models for the MAC values, more additional samples were necessary for infill than for frequencies. This can be explained by the fact that the response-surfaces of MAC values are more complex than those of frequencies. In particular, a transition region from a hinge to a fixed condition has a relatively large change rate.

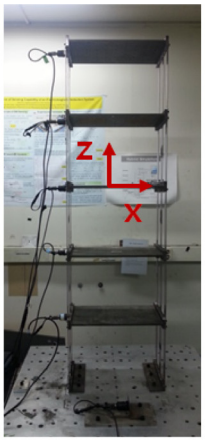

(a) Target structure

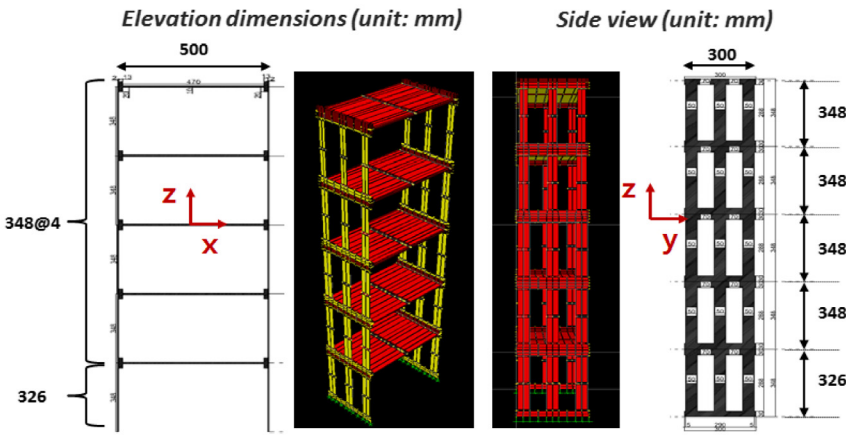

(b) Finite element model

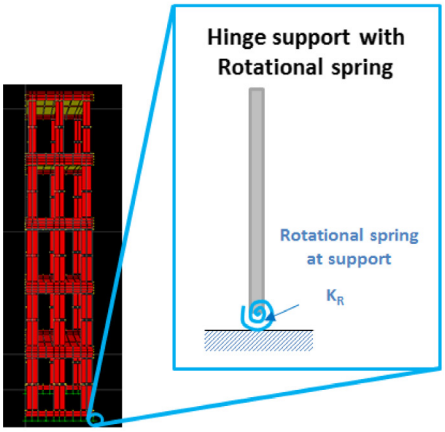

(c) Boundary condition with spring element

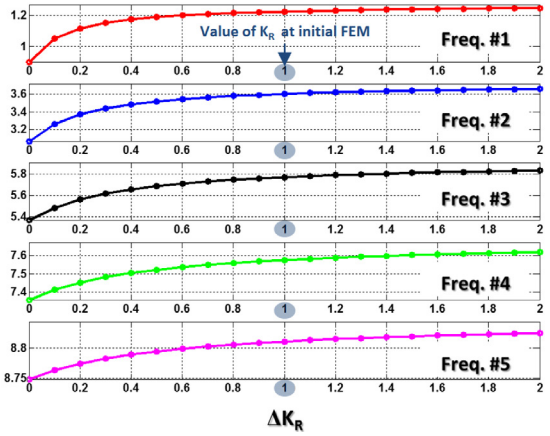

(d) Variation of boundary condition

Fig. 6. Target structure and finite element model.

Table 1
Structural properties used in the initial FE model.

Type	Mass density (kg/m^3)	Young's modulus (GPa)	Spring constant (N/rad)
Floor (shell element)	7904	196.1	–
Columns (shell element)	7600	196.1	–
Boundary condition (spring element)	–	–	19.61

Table 2
Result of identified parameter in numerical study.

Updating parameter	$\Delta X_{initial}$	ΔX_{Target}	$\Delta X_{Updated}$
Young's moduli of columns (E)	1	0.9	0.895
Rotational spring at support (K_R)	1	0.25	0.262

Prior to applying the Kriging models to FE model updating, 100 additional test samples were generated using uniformly distributed pseudo-random sampling, in order to emphasize the performance of the proposed method. Based on these additional samples, the R^2 and RMSE values were computed using FE analysis and the Kriging models. These are presented in Fig. 9, and we find the sufficient accuracies were achieved for all target modal properties.

FE model updating was carried out based on the constructed Kriging models. The objective function for FE model updating is formulated in terms of the discrepancy, as the weighted sum of the two sub-objective functions shown in Eq. (27).

$$J = \sum_i \omega_i^f \left(\frac{f_i^{CAL} - f_i^{EXP}}{f_i^{EXP}} \right)^2 + \sum_i \omega_i^{MAC} \left(\frac{(1 - \sqrt{MAC_i})^2}{MAC_i} \right)$$
$$\text{subject to } \sum_i \left(\omega_i^f + \omega_i^{MAC} \right) = 1, \quad \omega_i^f, \omega_i^{MAC} \geqslant 0 \tag{27}$$

where f_i^{CAL} and f_i^{EXP} denote the ith natural frequencies from the prediction (i.e., the Kriging model) and the experiment, respectively; MAC_i is the MAC value between the ith mode shapes from the prediction and the experiment; and ω_i^f and ω_i^{MAC} are weighting factors for the natural frequencies and MAC values, respectively, to condense Eq. (27) into a scalar value. FE model updating uses an optimization technique to minimize the scalar value of J. The objective function is formulated with the first three modal properties. The same weighting factors are assigned to each modal property. In this study, the genetic algorithm (GA) is employed for FE model updating. GA has the capability of global search based on the population, so it can indirectly evaluate the accuracy of the Kriging model over the whole parameter space. In order to improve the solution obtained by GA, the Nelder–Mead downhill simplex algorithm is applied.

The results of the FE model updating are summarized in Tables 2 and 3. FE model updating based on the proposed method was successful in identifying the correct value, and the relative errors of all natural frequencies were less than 0.3% with the perfect correlations of mode-shape. In particular, it was successful in updating the fourth and fifth modal properties, although these properties were not used in the formulation of the objective function. This numerical study indicates that the proposed method is successful to substitute the surrogate model to the iterative FE analysis in FE model updating. The computational efficiency of the proposed method is discussed in Section 3.4.

3.3. Experimental study

3.3.1. Dynamic testing of the target structure

We perform forced vibration testing using base-excitation, in order to excite the target structure and achieve a high signal-to-noise ratio. A shaking table is used to generate random excitation with a bandwidth from 0 to 20 Hz, because the maximum target frequencies of the initial FE model are under 10 Hz. A seismic accelerometer (PCB 393B12) with a magnetic tip was installed for each floor, as shown in Fig. 6a. A laptop computer was used as the data acquisition system, with a signal conditioner (PCB Model 481A03), a terminal block (NI BNC-2090), and a 16-bit

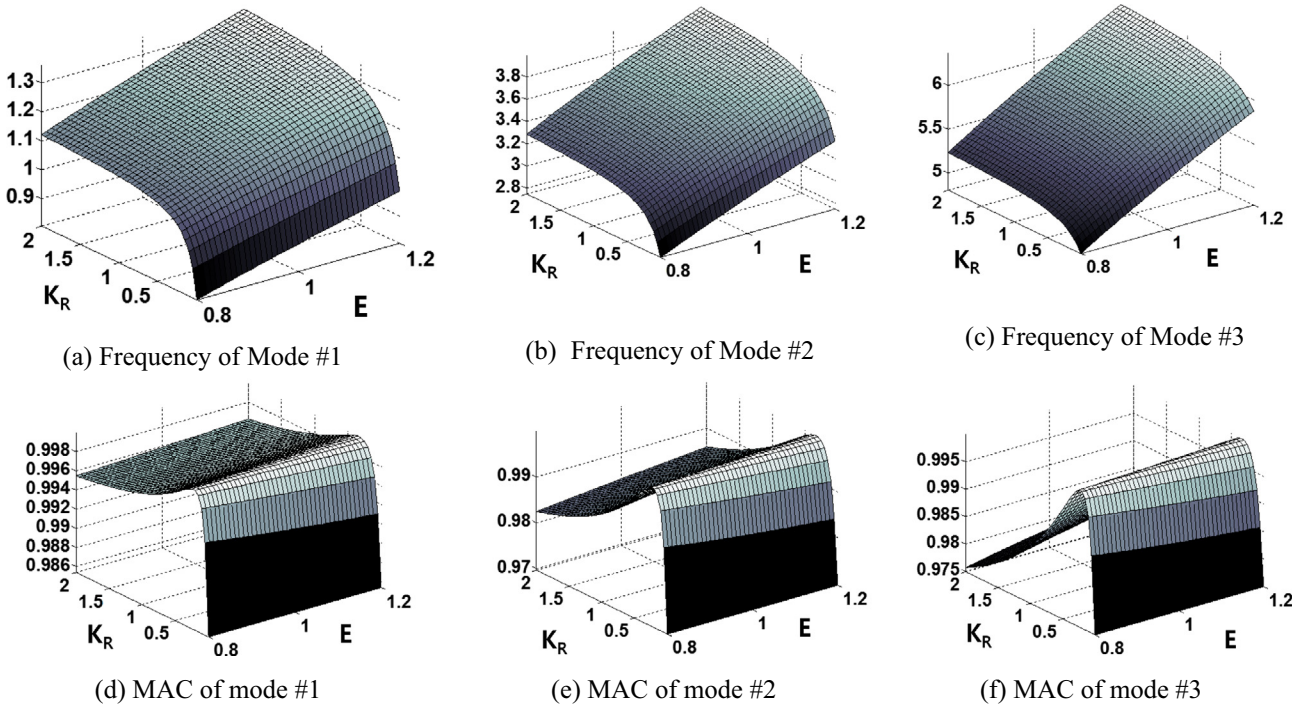

(a) Frequency of Mode #1 (b) Frequency of Mode #2 (c) Frequency of Mode #3

(d) MAC of mode #1 (e) MAC of mode #2 (f) MAC of mode #3

Fig. 7. Response-surfaces of FE model under perturbation of E (x-axis) and K_R (y-axis).

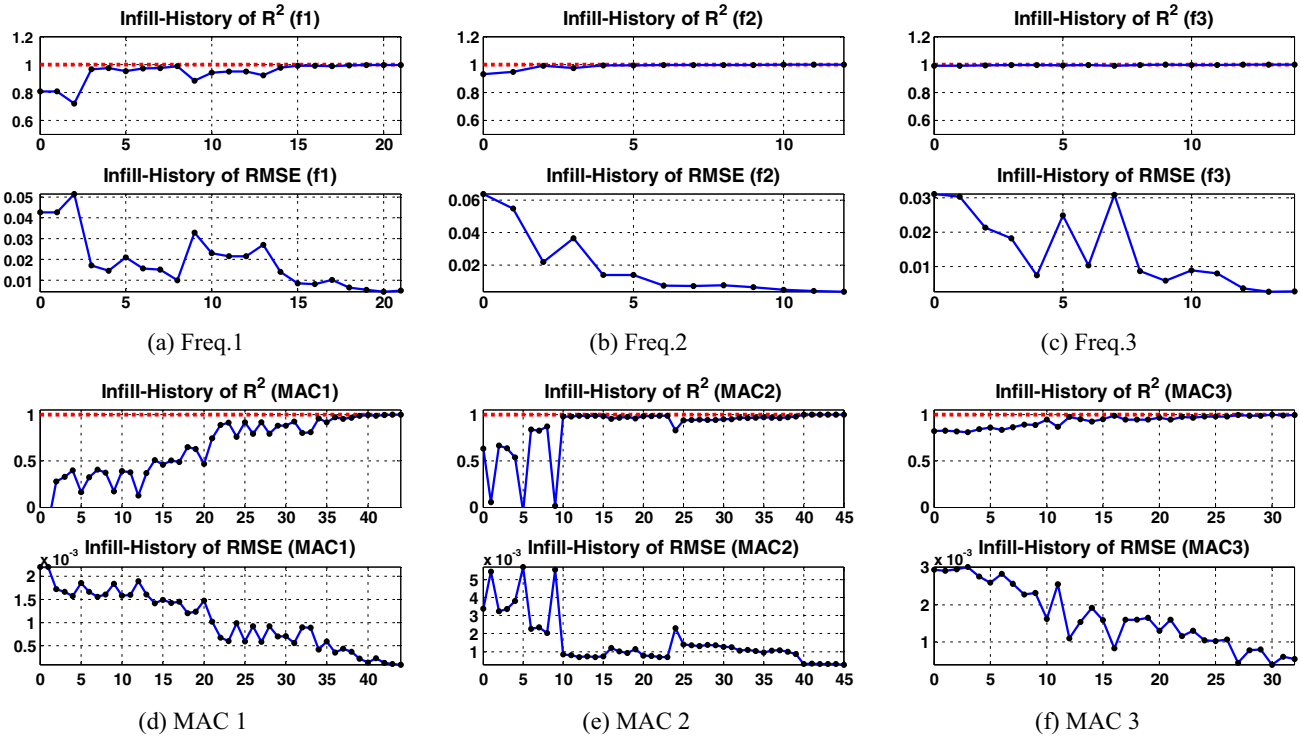

Fig. 8. Convergence of R^2 and RMSE: constructed from the 10 initial samples independently, *x*-axis: # infill, *y*-axis: validation metrics (top: R^2 and bottom: RMSE).

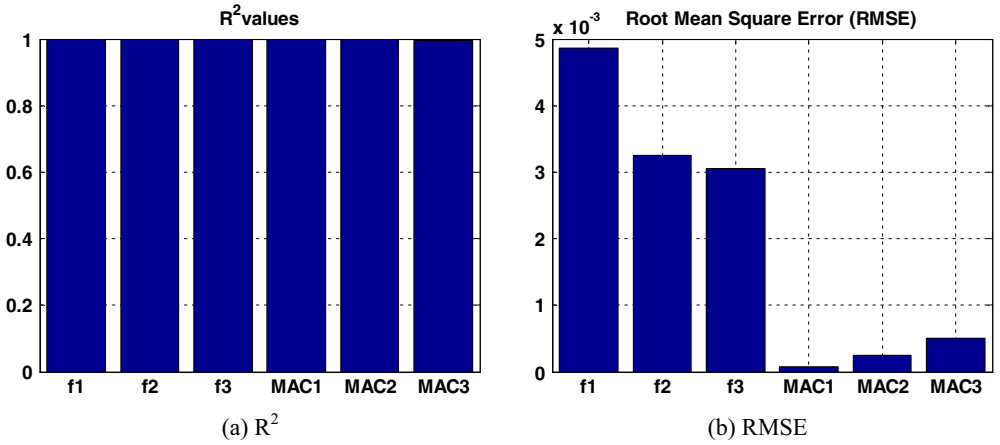

Fig. 9. R^2 and RMSE values of Kriging models based on 100 additional test samples.

Table 3
FE model updating result of numerical study.

Mode	f^{Target} (Hz)	Initial FE model			Updated FE model (Kriging model)		
		$f^{Initial}$ (Hz)	Relative error (%)	MAC	$f^{Updated}$ (Hz)	Relative error (%)	MAC
B1	1.085	1.224	12.82	0.998	1.086	−0.10	1
B2	3.250	3.602	10.81	0.991	3.250	−0.02	1
B3	5.318	5.771	8.52	0.989	5.310	−0.15	1
B4	7.093	7.576	6.81	0.992	7.077	−0.23	1
B5	8.330	8.810	5.76	0.998	8.308	−0.27	1

analog-to-digital converter (NI DAQCard-6036E). The accelerations of the five floors were measured for 10 min, with a sampling rate of 200 Hz. Fig. 10 presents the first singular values of frequency domain decomposition (FDD) and the stable poles of covariance-driven stochastic subspace identification (COV-SSI) from the dynamic testing. The five identified natural frequencies and their corresponding mode shapes are described in Fig. 11.

In Table 5, the modal properties identified from the initial FE model are compared with the modal properties identified using COV-SSI. The relative errors of the frequencies range from

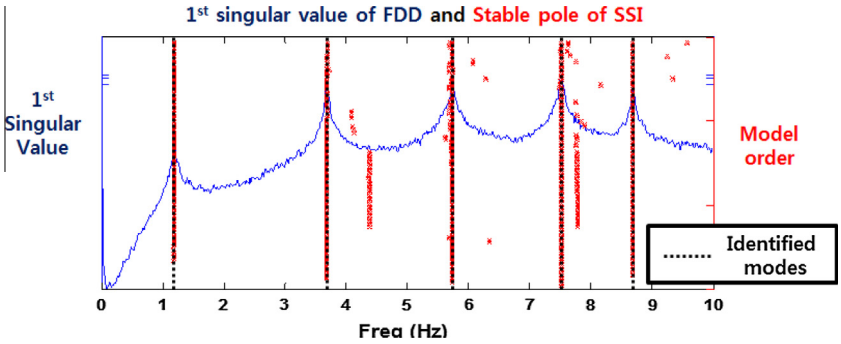

Fig. 10. Dual plot of the identified first singular value (FDD) and stabilization chart (SSI/COV).

−2.22% to 3.25%, while the MAC values range from 0.93 to 0.99. The three lowest frequencies are used to formulate the objective function (Eq. (27)) for the FE model updating, while the fourth and fifth modal properties are used to validate the identified results.

3.3.2. Selection of updating parameters

In a shear building structure, the mass property of each floor and stiffness property of each column are significantly influenced to the modal properties. If both the mass and stiffness properties are selected for each floor and column as the updating parameters, then the solution is not unique, resulting from mass and stiffness compensation in the modal properties. Therefore, we select Young's modulus for each column as one of the major updating parameters, under the assumption that the mass property for each floor is reasonably accurate. The mass property for each column and stiffness property for each floor are excluded from the updating parameters owing to their negligible contributions to the modal properties. In addition, the structural components with high degrees of uncertainty are potential updating parameters, so the rotational spring constant at the boundary condition is selected. The sizes and thicknesses of structural components are not considered, because the variability of their values is not significant. Therefore, six updating parameters were considered, as represented graphically in Fig. 12. In order to obtain physically meaningful values for the identified parameters, the ranges of the updating parameters were set to $0.8 \leqslant \Delta E_i \leqslant 1.2$ and $0.001 \leqslant \Delta K_R \leqslant 2$, based on engineering judgments and previous studies [3,5,41].

We performed a sensitivity analysis using the initial FE model in order to evaluate the influence of the selected updating parameters on the five identified natural frequencies. The first-order local sensitivity coefficient ($\hat{\boldsymbol{s}}_i$) was calculated using the finite difference

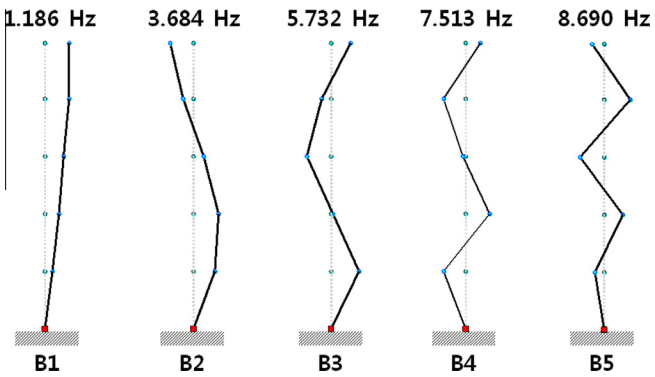

Fig. 11. Five identified modal properties.

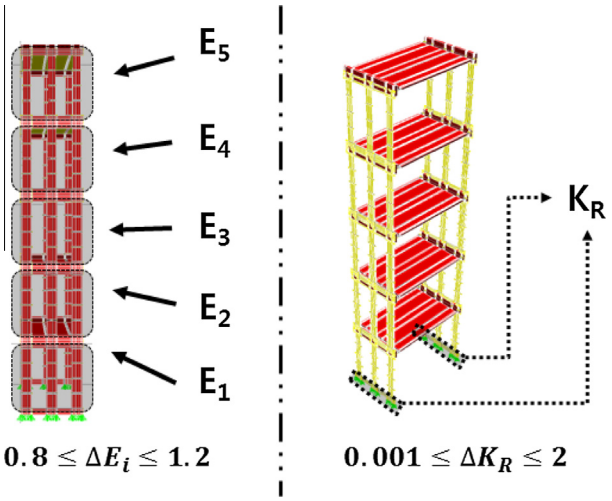

Fig. 12. Description of updating parameters.

method. The finite difference method for $\hat{\boldsymbol{s}}_i$ can be evaluated at a specific base point $(p_1^*, \ldots, p_i^*, \ldots, p_n^*)$ in the parameter space using the partial derivative of the target outputs $\boldsymbol{\lambda}$ with respect to one updating parameter (p_i), as

$$\hat{\boldsymbol{s}}_i = \left(\frac{\partial \boldsymbol{\lambda}}{\partial p_i}\right)_{(p_1^*,\ldots,p_n^*)} = \frac{\boldsymbol{\lambda}(p_1^*, \ldots, p_i^* + \Delta p_i, \ldots, p_n^*) - \boldsymbol{\lambda}(p_1^*, \ldots, p_i^*, \ldots, p_n^*)}{\Delta p_i} \tag{28}$$

The computed first-order local sensitivity of each updating parameter was calculated, and is plotted by a stacked bar chart in Fig. 13.

The sensitivities of the Young's moduli (E_1–E_5) are sufficient for affecting the first three modal properties. Their sensitivities exhibit linear behavior at the lower and upper bounds, because the ratios at each modal property are consistent, as shown in Fig. 13. In contrast, the rotational spring at the support (K_R) mostly affects the lower natural frequencies at lower bounds. At upper bounds, the contributions of the modal properties are comparatively smaller than those of the Young's moduli. In this regard, the sensitivity behaves non-linearly at the lower and upper bounds. In summary, the selected updating parameters show a considerable effect on the identified modal properties, and it is expected that the response-surfaces will be a lot more complicated than in the case of the numerical study presented in Section 3.2.

3.3.3. Model updating based on experimental data

We generated 60 samples by using optimized LHS to construct an initial Kriging model. For the validation data set, 100 samples

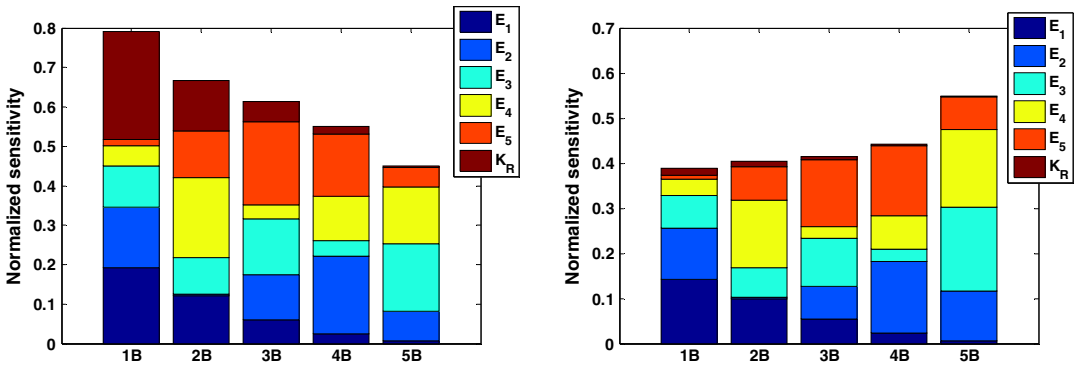

(a) Lower bounds (b) Upper bounds

Fig. 13. Normalized sensitivities of updating parameters at the lower and upper bounds.

were generated by optimized LHS to evaluate the accuracy of the Kriging model with the proposed stopping criteria. Six Kriging models were constructed using the proposed method, under 0.98 and 0.01 of the thresholds of R^2_{Th} and $\Delta RMSE_{Th}$, respectively. The proposed method was carried out based on a sequential use of the training samples (detailed in Section 3.4), from the first natural frequencies to the MAC of the five modal properties in alphabetical order, as presented in Fig. 14. Further details on this sequential use of the training samples are described in Section 3.4. The total number of iterations of the FE analysis was 274 in the experimental study. This consisted of 60 initial samples, 114 infill samples, and 100 validation samples.

Similar to Section 3.2, 400 samples were generated independently, using uniformly distributed pseudo-random sampling, in order to emphasize the performance of the proposed method. We note that this additional validation is not required for real implementation. The R^2 and RMSE values based on the randomly generated samples were computed, and are shown in Fig. 15. It can be seen that the Kriging models of all modal properties accurately reproduce the target modal properties.

FE model updating based on the identified modal properties was performed, in a similar manner as in Section 3.2. In this study the weighting factors are assigned as [1 1 1 1 1 1] for $\left[\omega_1^f\ \omega_2^f\ \omega_3^f\ MAC_1\ MAC_2\ MAC_3\right]$, for the sake of simplicity. Regarding the concept of residual minimization, the result of the FE model updating should minimize the discrepancy between the experimental and updated modal properties (i.e., the first three natural frequencies and MAC values).

A comparison between the modal properties of the identified and updated values following FE model updating is presented in Table 4. The results of the FE model updating based on the proposed method are summarized in Table 5. The first three updated natural frequencies (i.e., 1st–3rd) showed significant improvement in attaining values closer to the identified values. Considering that the first three modal properties were used to formulate the objective function, the updated FE model should reproduce these three modal properties accurately. In this regard, FE model updating based on the proposed method is successful in updating the initial FE model. This implies that the Kriging model works well as a substitute for the iterative FE analysis.

However, the updated fourth and fifth natural frequencies deviate more from those of the initial FE model. This can be explained by the fact that these modal properties (i.e., 4th–5th) were not used in the formulation of the objective function. In the absence of modeling errors and measurement uncertainty, these modal properties must be updated to the identified values, which give the same results as the numerical study (Table 3). Unfortunately, in reality, it is inevitable to remove the model errors and uncertainties in the identified measurements. Therefore, the conventional residual minimization method (Eq. (27)) forced the FE model updating to fit the identified modal properties (i.e., calibrated data), although these identified modal properties may be contaminated or biased owing to modeling errors and measurement uncertainties. Accordingly, non-deterministic FE model updating has been developed in order to consider modeling errors and measurement uncertainty. In general, a large number of the iterative FE analyses are required to generate statistical/probable samples for probabilistic simulations, such as the Markov chain Monte Carlo (MCMC) method; however, this approach remains computationally heavy.

Based on the results of FE model updating and the additional validation test (i.e., 400 random samples), it can be concluded that the proposed method is successful in replacing the iterative FE analysis. Before closing this section, we note that the proposed method can be easily extended to real-scaled structures and various applications, including non-deterministic FE model updating and reliability analysis with a multiple limit state function.

3.4. Discussion on computational efficiency and practical implementation

In order to evaluate the required computational effort, we used an Intel(R) Xeon(R) E5-2660 v2 processor, running with 2.20 and 2.90 GHz, 16 GB RAM, and the Windows7 OS. Before discussing the computational efficiency, we will describe the practical implementation of the proposed method. Considering that the modal properties are calculated simultaneously from FE analysis, all target modal properties can be obtained simultaneously, and we apply the training samples sequentially. In order to demonstrate the sequential implementation of the training samples, we applied the proposed method to a numerical study. This is shown in Fig. 16, and described as follows:

1. For the first natural frequency, the 30 infill samples are added using the proposed method. Once each infill sample is evaluated by FE analysis, all modal properties (three frequencies and three MAC values) are obtained and stored.
2. The proposed method begins with the 40 training samples (10 initial samples +30 infill samples) from step 1 for the second natural frequency. In this step, only one infill is added.
3. The proposed method is sequentially applied to the remainder of the modal properties. Finally, a total number of 47 training samples are added as the infill.

Therefore, the total number of iterations of the FE analysis is 97, consisting of 10 initial samples, 47 infill samples, and 40 validation

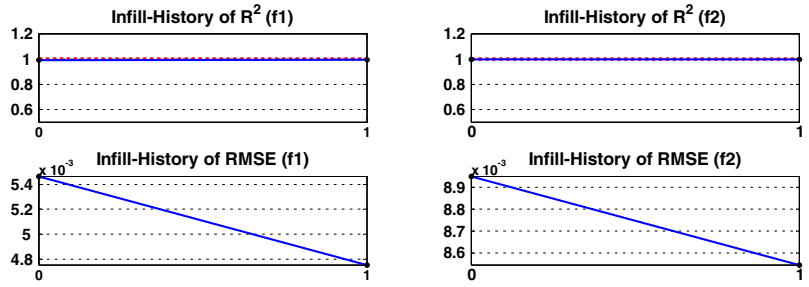

(a) Freq.1

(b) Freq.2

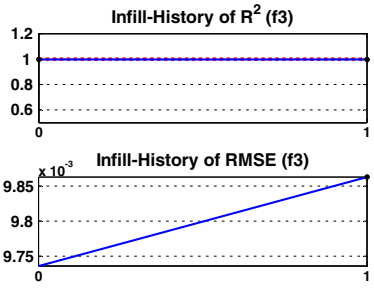

(c) Freq.3

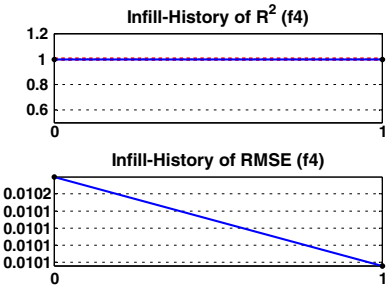

(d) Freq.4

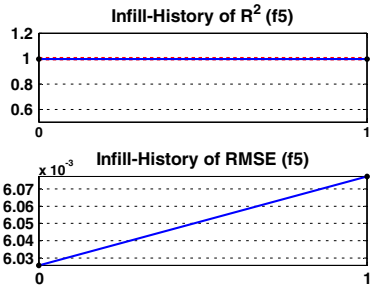

(e) Freq.5

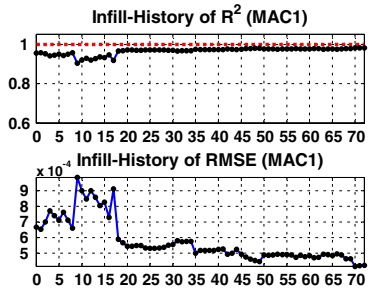

(f) MAC1

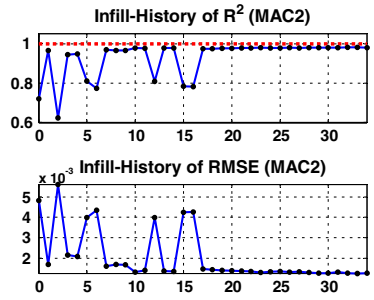

(g) MAC2

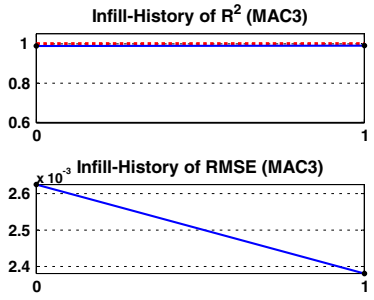

(h) MAC3

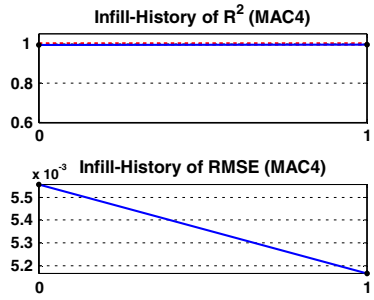

(i) MAC4

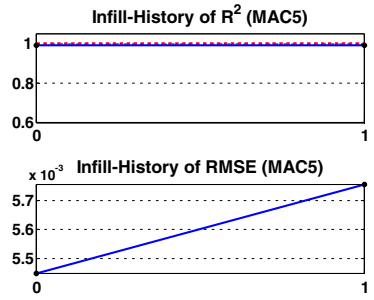

(j) MAC5

Fig. 14. Convergence of R^2 and RMSE: The sequential use of the training samples from Freq. 1 to MAC 5, *x*-axis: # infill, *y*-axis: validation metrics (top: R^2 and bottom: RMSE).

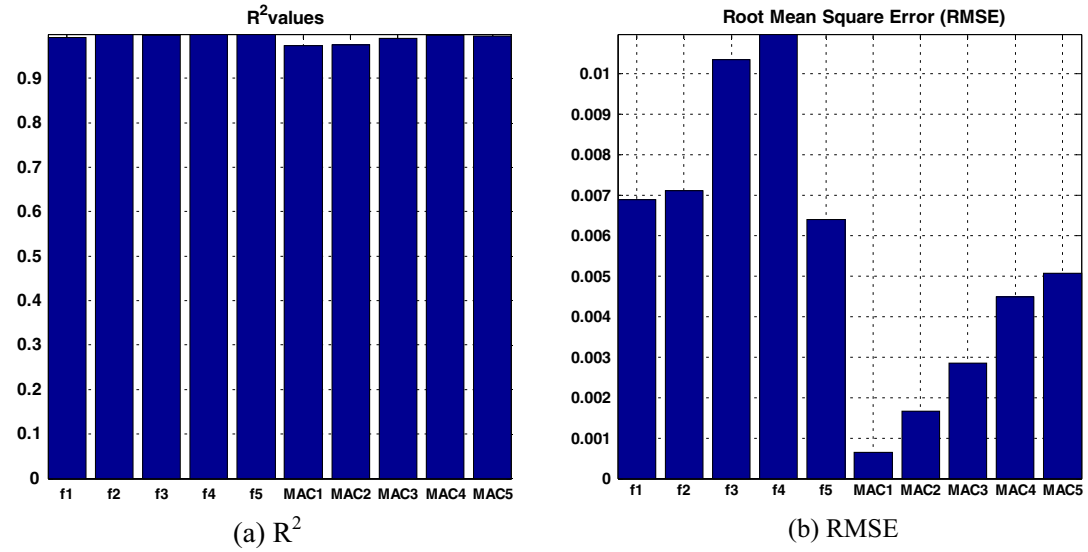

(a) R^2 (b) RMSE

Fig. 15. R^2 and RMSE values of Kriging models based on 400 additional test samples.

Table 4
Result of identified parameter in experimental study.

Updating parameter	$\Delta X_{initial}$	$\Delta X_{Updated}$
E_1	1	0.93
E_2	1	0.81
E_3	1	0.94
E_4	1	1.15
E_5	1	1.09
K_R	1	1.50

Table 5
FE model updating result of experimental study.

Mode	f^{Target} (Hz)	Initial FE model			Updated FE model (Kriging model)		
		$f^{Initial}$ (Hz)	Relative error (%)	MAC	$f^{Initial}$ (Hz)	Relative error (%)	MAC
B1	1.186	1.224	3.25	0.999	1.184	−0.10	0.999
B2	3.684	3.062	−2.22	0.992	3.692	0.22	0.997
B3	5.732	5.771	0.68	0.975	5.744	0.21	0.997
B4	7.513	7.576	0.84	0.933	7.380	−1.77	0.991
B5	8.690	8.810	1.39	0.942	8.904	2.47	0.987

samples. We checked that the FE model updating using these Kriging models was successful in identifying the true value for the numerical study.

In order to investigate the computational costs for the direct FE analysis and the proposed method, the total number of the FE analysis during FE model updating of the experimental study is estimated. Both approaches require around 5300 function evaluations for GA (5400 for the direct FE analysis and 5200 for the surrogate models), and around 350 function evaluations for NM (312 for direct FE analysis and 396 for the surrogate models). The average time needed for the Kriging prediction for each modal property ranges from about 2.323e−4 to 2.531e−4 s, so that the total average time is estimated to be about 1.4e−3 s, by the summation of those needed for each of the six modal properties. On the other hand, the average time needed to compute all of the modal properties at once in the direct FE analysis is about 10.543 s (except for the computational time for the three MAC values). As demonstrated in Section 3.3.3, the total number of the required FE analysis with the surrogate model is 274. A comparison between the computational costs for the direct and proposed method is presented in Table 6. This indicates that the proposed method is considerably more computationally efficient than the direct approach (i.e., the FE model). Considering that the FE model used in this study is not very computationally extensive, the computational efficiency in FE model updating is expected to be improved significantly using a high-fidelity FE model and a sophisticated updating algorithm (e.g., MCMC).

Finally, we note that surrogate modeling is not always required in FE model updating. However, the use of the surrogate model would be more practical than a direct FE analysis in some situations (e.g., with limited resources or time constraints). When sophisticated modeling or finer FE discretization with full geometric description (a high-fidelity model) is used to minimize systematic errors (i.e., modeling and discretization errors), the computational cost increases. Depending on the modeling, such high-fidelity modeling can increase the required computational time from seconds to minutes for a simple analysis (e.g., a modal analysis). For a single run, this would not be demanding. However, if the numerical simulation will be iterated many times, the computational cost would become very demanding with limited resources or time constraints. This computational issue can be addressed by either high performance computing (HPC) (such as parallel or distributed computing) or the use of surrogate modeling. In general, HPC is not always possible, owing to computational and message passing interface programming requirements. In such cases, surrogate modeling can provide an alternative solution for addressing computational issues in FE model updating using a high-fidelity model. In this context, the proposed method can be customized for a variety of the response-surfaces and useful for a less experienced user with surrogate modeling for FE model updating.

4. Conclusions

In this study, we have proposed a new method for more robust and flexible surrogate modeling for FE model updating. Based on our existing knowledge and a literature survey, the previous investigations on surrogate modeling for FE model updating have proceeded on the basis of the classical design of experiments. In such methods, the generated training samples are used identically for all target outputs in order to build surrogate models at once. In addition, a trial-and-error approach is required, since the response-surfaces are not known beforehand. Therefore, this iterative

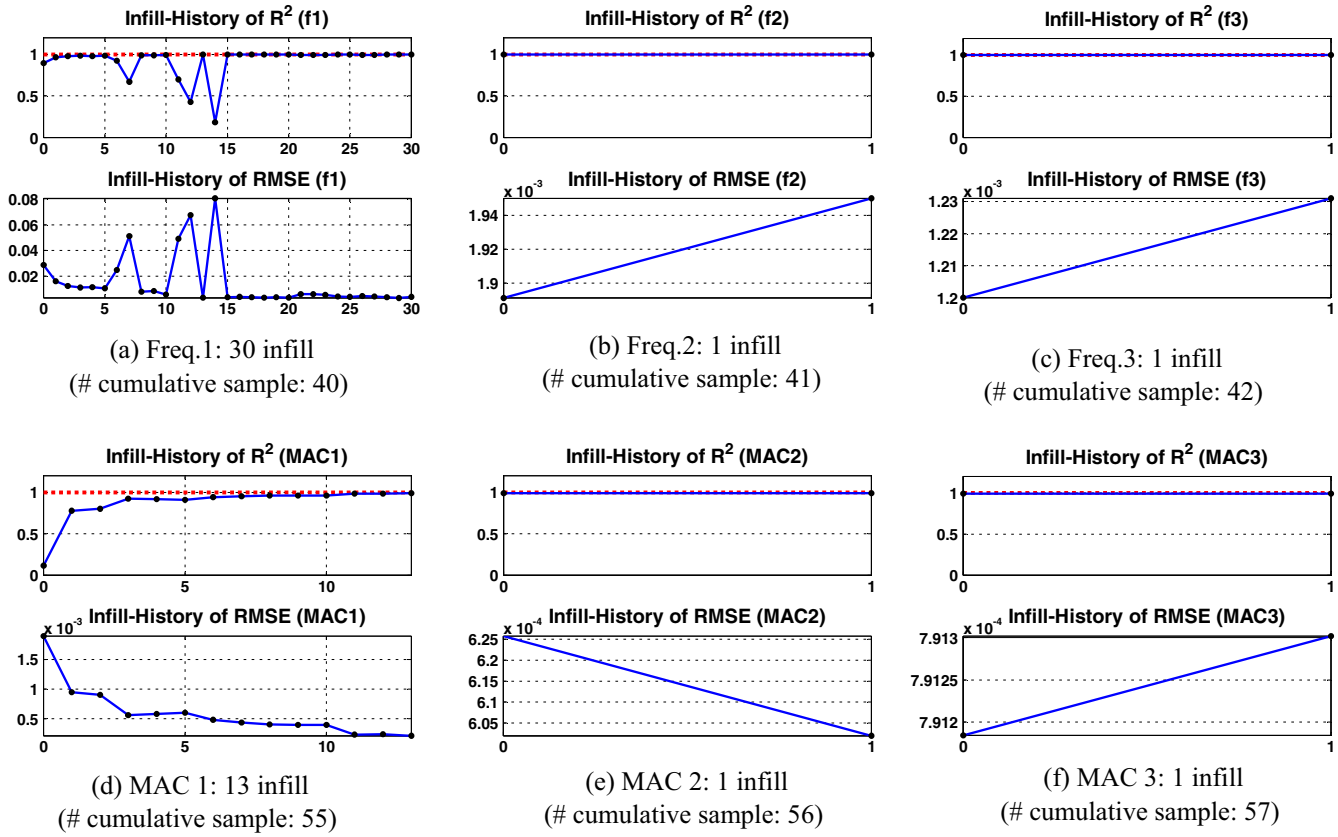

(a) Freq.1: 30 infill (# cumulative sample: 40)

(b) Freq.2: 1 infill (# cumulative sample: 41)

(c) Freq.3: 1 infill (# cumulative sample: 42)

(d) MAC 1: 13 infill (# cumulative sample: 55)

(e) MAC 2: 1 infill (# cumulative sample: 56)

(f) MAC 3: 1 infill (# cumulative sample: 57)

Fig. 16. The sequential use of the training samples: numerical study *x*-axis: # infill, *y*-axis: validation metrics (top: R^2 and bottom: RMSE).

Table 6
Comparison for the computational efficiency (unit: seconds).

	Surrogate modeling	FE model updating		Estimated total time
		Genetic algorithm	Nelder-Mead downhill simplex	
Direct FE model-based	0	56932.20 (5400 × 10.543 FEA)[a]	3289.42 (312FEA × 10.543 FEA)[a]	60221.62
Surrogate model-based	2888.78 (274 × 10.543 FEA)	7.28 (5200 × 0.0014 SURRO)[b]	0.55 (396SURRO × 0.0014 SURRO)[b]	2896.61

[a] FE analysis.
[b] Surrogate model.

method is subjective, and so it is sometimes challenging to secure reasonable accuracy in the surrogate model.

As illustrated in Figs. 7 and 8, FE model may exhibit different response-surfaces, ranging from simple and smooth to complex surfaces, even for identical input parameters (i.e., due to different sensitivity). As a result, the required number of the training samples may be different. In this situation, the use of the identical training samples to all target outputs cannot capture these characteristics and it is difficult to find the adequate training samples (i.e., locations and sample size).

In order to address these difficulties, we have introduced a sequential surrogate modeling based on a statistical interpretation of the Kriging model. The fundamental concept of applying the sequential surrogating modeling is not entirely new to global optimization. However, the sequential surrogate modeling is somewhat new for FE model updating. As shown in Fig. 4a, the sequential surrogate modeling strategy in global optimization is not adequate for FE model updating. Therefore, we modified and proposed the sequential surrogate modeling for FE model updating. In order to evaluate the effectiveness of the proposed method when applied to FE model updating, we performed numerical and experimental investigations by using a five-story shear building model. It was demonstrated both numerically and experimentally that the Kriging model using the proposed method can be a successful substitute for an iterative FE analysis. Therefore, we concluded that Kriging model-based FE model updating using a sequential surrogate modeling shows promise for building an accurate surrogate model automatically and flexibly for a variety of the response-surfaces, with minimal user intervention and a tremendous computational efficiency.

Acknowledgement

This research was partially supported by a grant (13SCIPA01) from Smart Civil Infrastructure Research Program funded by Ministry of Land, Infrastructure and Transport (MOLIT) of Korea government and Korea Agency for Infrastructure Technology Advancement (KAIA) and Basic Science Research Program through the National Research Foundation of Korea (NRF) funded by the Ministry of Education (2013R1A1A2011351).

References

[1] Catbas FN, Kijewski-Correa TL, Aktan AE. Committee on structural identification of constructed systems. In: Structural identification of constructed systems: approaches, methods, and technologies for effective practice of St-Id2013. Structural Engineering Institute; 2013.

[2] Baruch M. Optimization procedure to correct stiffness and flexibility matrices using vibration tests. AIAA J 1978;16:1208–10.
[3] Brownjohn JMW, Xia PQ, Hao H, Xia Y. Civil structure condition assessment by FE model updating: methodology and case studies. Finite Elem Anal Des 2001;37:761–75.
[4] Mottershead JE, Link M, Friswell MI. The sensitivity method in finite element model updating: a tutorial. Mech Syst Signal Process 2011;25:2275–96.
[5] Jin SS, Cho S, Jung HJ, Lee JJ, Yun CB. A new multi-objective approach to finite element model updating. J Sound Vib 2014;333:2323–38.
[6] Beck JL, Katafygiotis LS. Updating models and their uncertainties. I: Bayesian statistical framework. J Eng Mech-ASCE 1998;124:455–61.
[7] Beck JL, Au SK. Bayesian updating of structural models and reliability using Markov chain Monte Carlo simulation. J Eng Mech-ASCE 2002;128:380–91.
[8] Ching JY, Chen YC. Transitional markov chain monte carlo method for Bayesian model updating, model class selection, and model averaging. J Eng Mech-ASCE 2007;133:816–32.
[9] Cheung SH, Beck JL. Bayesian model updating using hybrid Monte Carlo simulation with application to structural dynamic models with many uncertain parameters. J Eng Mech-ASCE 2009;135:243–55.
[10] Yuen KV, Kuok SC. Bayesian methods for updating dynamic models. Appl Mech Rev 2011;64.
[11] Nichols JM, Moore EZ, Murphy KD. Bayesian identification of a cracked plate using a population-based Markov Chain Monte Carlo method. Comput Struct 2011;89:1323–32.
[12] Goulet J-A, Texier M, Michel C, Smith IFC, Chouinard L. Quantifying the effects of modeling simplifications for structural identification of bridges. J Bridge Eng 2014;19:59–71.
[13] Eamon CD, Nowak AS. Effect of secondary elements on bridge structural system reliability considering moment capacity. Struct Saf 2004;26:29–47.
[14] Steenackers G, Guillaume P. Finite element model updating taking into account the uncertainty on the modal parameters estimates. J Sound Vib 2006;296:919–34.
[15] Goulet JA, Smith IFC. Structural identification with systematic errors and unknown uncertainty dependencies. Comput Struct 2013;128:251–8.
[16] Ren WX, Chen HB. Finite element model updating in structural dynamics by using the response surface method. Eng Struct 2010;32:2455–65.
[17] Marwala T. Finite element model updating using response surface method. In: Collection of technical papers AIAA/ASME/ASCE/AHS/ASC structures, structural dynamics and materials conference; 2004. p. 7.
[18] Deng L, Cai CS. Bridge model updating using response surface method and genetic algorithm. J Bridge Eng 2010;15:553–64.
[19] Fang SE, Perera R. Damage identification by response surface based model updating using D-optimal design. Mech Syst Signal Process 2011;25:717–33.
[20] Ren WX, Fang SE, Deng MY. Response surface-based finite-element-model updating using structural static responses. J Eng Mech-ASCE 2011;137:248–57.
[21] Chakraborty S, Sen A. Adaptive response surface based efficient finite element model updating. Finite Elem Anal Des 2014;80:33–40.
[22] Zhou LR, Yan GR, Ou JP. Response surface method based on radial basis functions for modeling large-scale structures in model updating. Comput-Aided Civ Inf 2013;28:210–26.
[23] Wan HP, Ren WX. A residual-based Gaussian process model framework for finite element model updating. Comput Struct 2015;156:149–59.
[24] Jones DR. A taxonomy of global optimization methods based on response surfaces. J Glob Optim 2001;21:345–83.
[25] Forrester AIJ, Sóbester As, Keane AJ. Engineering design via surrogate modelling: a practical guide. Chichester, West Sussex, England; Hoboken, NJ: J. Wiley; 2008.
[26] Krige DG. A statistical approach to some basic mine valuation problems on the witwatersrand. J S Afr Inst Min Metall 1994;94:95–111.
[27] Theil H. Principles of econometrics. New York: Wiley; 1971.
[28] Sacks J, Welch WJ, Mitchell TJ, Wynn HP. Design and analysis of computer experiments. Stat Sci 1989;4:409–23.
[29] Locatelli M. Bayesian algorithms for one-dimensional global optimization. J Glob Optim 1997;10:57–76.
[30] Bastos LS, O'Hagan A. Diagnostics for Gaussian process emulators. Technometrics 2009;51:425–38.
[31] Morris MD, Mitchell TJ. Exploratory designs for computational experiments. J Stat Plan Infer 1995;43:381–402.
[32] Queipo NV, Haftka RT, Shyy W, Goel T, Vaidyanathan R, Tucker PK. Surrogate-based analysis and optimization. Prog Aerosp Sci 2005;41:1–28.
[33] Damblin G, Couplet M, Iooss B. Numerical studies of space-filling designs: optimization of latin hypercube samples and subprojection properties. J Simul 2013;7:276–89.
[34] Vu-Bac N, Silani M, Lahmer T, Zhuang X, Rabczuk T. A unified framework for stochastic predictions of mechanical properties of polymeric nanocomposites. Comput Mater Sci 2015;96:520–35.
[35] Sobol IM, Asotsky DI. One more experiment on estimating high-dimensional integrals by quasi-Monte Carlo methods. Math Comput Simul. 2003;62:255–63.
[36] Vu-Bac N, Lahmer T, Keitel H, Zhao J, Zhuang X, Rabczuk T. Stochastic predictions of bulk properties of amorphous polyethylene based on molecular dynamics simulations. Mech Mater 2014;68:70–84.
[37] Vu-Bac N, Lahmer T, Zhang Y, Zhuang X, Rabczuk T. Stochastic predictions of interfacial characteristic of polymeric nanocomposites (PNCs). Compos Part B-Eng 2014;59:80–95.
[38] Jones DR, Schonlau M, Welch WJ. Efficient global optimization of expensive black-box functions. J Glob Optim 1998;13:455–92.
[39] Loeppky JL, Sacks J, Welch WJ. Choosing the sample size of a computer experiment: a practical guide. Technometrics 2009;51:366–76.
[40] Bennett ND, Croke BFW, Guariso G, Guillaume JHA, Hamilton SH, Jakeman AJ, et al. Characterising performance of environmental models. Environ Modell Softw 2013;40:1–20.
[41] Zhang QW, Chang CC, Chang TYP. Finite element model updating for structures with parametric constraints. Earthquake Eng Struct 2000;29:927–44.